Letters

Closed-Loop Precharge Control of Modular Multilevel Converters During Start-Up Processes

Binbin Li, Dandan Xu, Yi Zhang, Rongfeng Yang, Gaolin Wang, *Member, IEEE*, Wei Wang, and Dianguo Xu, *Senior Member, IEEE*

***Abstract*—This letter respectively presents two closed-loop precharge control methods to fully charge the submodule (SM) capacitors of the modular multilevel converter (MMC) during dc-side and ac-side start-up processes. The proposed methods are aimed at regulating a constant charging current thus reducing the start-up time and eliminating the inrush current. Besides, capacitor voltage balancing control is also embedded into the controller to equally charge the SM capacitors. Due to the flexibility of the closed-loop control, these methods are applicable to any MMC applications regardless of the number of SMs. Finally, effectiveness of the proposed methods is verified experimentally on a three-phase prototype of MMC.**

***Index Terms*—Closed-loop precharge control, modular multilevel converter (MMC), start-up scheme.**

I. Introduction

THE modular multilevel converter (MMC) is receiving increasing attentions in recent years due to its distinctive features compared with other topologies in medium- and high-voltage applications, such as scalability, high efficiency, low semiconductor stresses, excellent voltage waveform quality, reduced EMI noise, and enhanced reliability. These advantages make MMC particularly attractive for the fields of HVDC power transmission and medium-voltage drives [1]–[4]. During the last years, intensive studies have been carried out in the literatures to improve the performances of MMC [5]–[13], which mainly focused on mathematical analysis, modulation, fault detection, voltage balancing, circulating current suppression, and injection algorithms, etc.

Nevertheless, one specific but rarely mentioned issue associated with MMC is that the capacitors of the submodules (SMs) need to be precharged to nominal voltage value before getting into operation. Otherwise a large inrush current may occur at the instant of start, threatening the safe operation of the IGBTs and the capacitors, or even leading to the breakdown of the whole MMC system. For these reasons, a soft start-up process is necessary. One straightforward start-up method is to add an auxiliary power supply to the dc-bus bars of MMC, whose voltage is equal to one nominal SM capacitor voltage, then the SMs are inserted one by one to get charged [4], [14]. This method is very simple but not practical due to its high cost and inflexibility. To get rid of the auxiliary power supply, other start-up schemes were proposed to directly precharge the capacitors by absorbing power from the dc-side main voltage [15], [16], or from the ac-side main voltage [17]. In [15], the upper-arm and lower-arm SMs were inserted by turns to get charged by the dc-side main voltage. In a similar philosophy, [17] presented the start-up control method of a clamp double submodule (CDSM) based MMC by grouping the CDSMs and charging them group by group. But this method did not consider the most commonly used half-bridge SM structure, and can only apply to MMC with a great number of SMs (e.g., in HVDC applications), hence it is not suitable for MMC with a limited number of SMs (e.g., in medium-voltage applications). In addition, both [15] and [17] features an *RC* charging circuit, in which the charging current decayed exponentially and resulted in a longtime start-up process, which is unacceptable in some conditions especially when quick restart after temporary fault is required [8]. Another start-up scheme was proposed in [16], which charged the SMs by gradually decreasing the number of inserted SMs and the duty cycle of the pulse width modulation (PWM) SM. However, all of these existing methods are based on an open-loop approach, which means that the charging current during the start-up process is not controlled. Consequently, these methods quite rely on the circuit parameters and may lead to over current problems if unexpected disturbances or parameter variations occur.

In this letter, two closed-loop precharge control methods are proposed for MMC, respectively, with respect to start-up from the dc-side main voltage and from the ac-side main voltage. By means of feedback control, the charging current is regulated at a constant value thus the SM capacitors can be linearly charged, which significantly reduces the start-up time. Inherited from the easy implementation and robustness of closed-loop control, the proposed start-up methods have good immunity to parameter variations and are independent from the number of SMs, thereby applicable to any MMC application. Moreover, the voltage balancing control is also embedded to ensure the

Manuscript received February 20, 2014; revised June 8, 2014 and May 12, 2014; accepted June 25, 2014. Date of publication June 30, 2014; date of current version October 7, 2014. This work was supported by the National Natural Science Foundation of China (51237002) and by grants from the Power Electronics Science and Education Development Program of Delta Environmental and Educational Foundation. Recommended for publication by Associate Editor H. Chung.

The authors are with the School of Electrical Engineering and Automation, Harbin Institute of Technology, Harbin 150001, China (e-mail: libinbinhit@126.com; dan_danzai@163.com; zysean@163.com; yrf@hit.edu.cn; WGL818@hit.edu.cn; wangwei602@hit.edu.cn; xudiang@hit.edu.cn).

Color versions of one or more of the figures in this paper are available online at http://ieeexplore.ieee.org.

Digital Object Identifier 10.1109/TPEL.2014.2334055

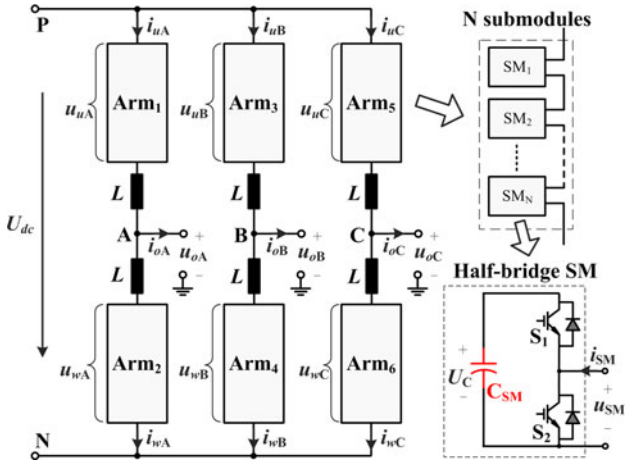

Fig. 1. Circuit configuration of the modular multilevel converter (MMC).

SM capacitor voltages are equally charged during the whole start-up process. Finally, effectiveness of the proposed methods is verified by experiments on a three-phase MMC prototype.

II. Basic Operating Principles and Uncontrolled Precharge Processes

A. SM Operating Principles

The circuit configuration of a three-phase MMC is shown in Fig. 1. Each phase of it consists of two arms, the upper and the lower, which are connected through two buffer inductors. Each arm is formed by a series connection of N nominally identical half-bridge SMs, and each SM contains a dc storage capacitor $C_{\rm SM}$ and two IGBTs (i.e., S_1 and S_2). Consequently, there are three possible working states in terms of each SM as follows:

1) *Inserted*: S_1 is switched on while S_2 is switched off. $C_{\rm SM}$ is connected to the arm. If the charging current $i_{\rm SM}$ is positive, then $C_{\rm SM}$ will get charged; otherwise, it will be discharged.
2) *Bypassed*: S_1 is switched off while S_2 is switched on. $C_{\rm SM}$ is disconnected from the arm and U_C will be kept constant.
3) *Blocked*: Both S_1 and S_2 are switched off. As a result, the working status of $C_{\rm SM}$ is determined by the direction of $i_{\rm SM}$. If $i_{\rm SM}$ is positive, $C_{\rm SM}$ will be charged through the free-wheeling diode of S_1; otherwise, $C_{\rm SM}$ is disconnected and U_C will be kept constant.

Note that if $C_{\rm SM}$ is paralleled with a bleeder resistor and will be disconnected from the arm for a long time (e.g., a few seconds), then it will still get discharged. Additionally, each SM requires a switching power supply to feed the driving circuit of the IGBTs, which also takes power from the local capacitor [18], [19].

B. Uncontrolled Precharge Process From the DC-Side Main Voltage

When the dc-terminal of MMC is connected with a dc power source (e.g., diode rectifier in motor drive application, or the dc

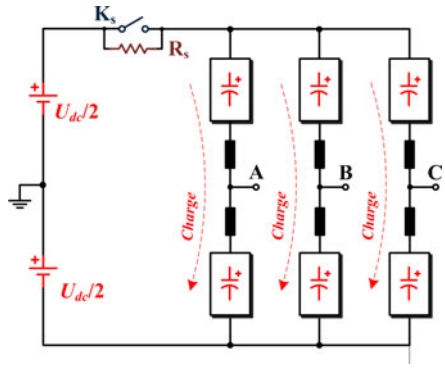

Fig. 2. Precharge from the dc-side main voltage.

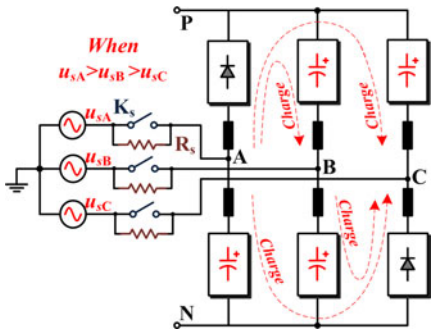

Fig. 3. Precharge from the ac-side main voltage.

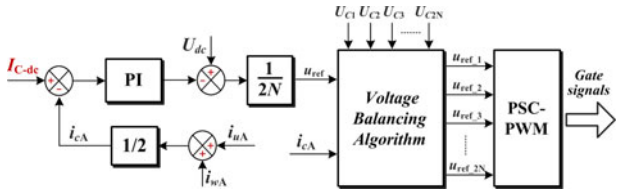

Fig. 4. Proposed closed-loop precharge method from the dc-side main voltage.

voltage of HVDC system), SM capacitors will be automatically precharged in an uncontrolled process, as shown in Fig. 2, where a resistor–contactor arrangement is used to limit the inrush current into the capacitors. This process is uncontrollable because the capacitor voltages are not high enough to drive the IGBTs, and the SMs are in blocked mode. Thus, the SM capacitors will be charged through the free-wheeling diode of S_1. As there are totally $2N$ SMs in one phase of the charging path, the maximum attainable capacitor voltage during this process can be obtained as

$$U_{C(\rm initial)} = \frac{U_{\rm dc}}{2N}. \tag{1}$$

For normal operation of MMC, the rated SM capacitor voltage $U_{C(\rm rated)}$ should equal to one Nth of the dc main voltage, that is $U_{\rm dc}/N$. Hence, (1) can be rewritten as

$$U_{C(\rm initial)} = \frac{U_{C(\rm rated)}}{2}. \tag{2}$$

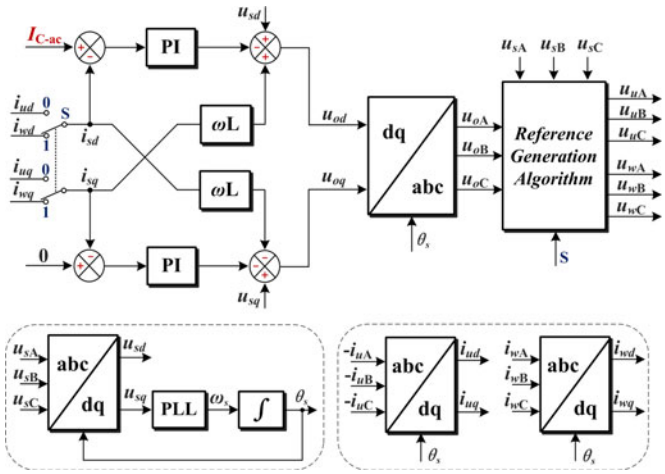

Fig. 5. Proposed closed-loop precharge method from the ac-side main voltage.

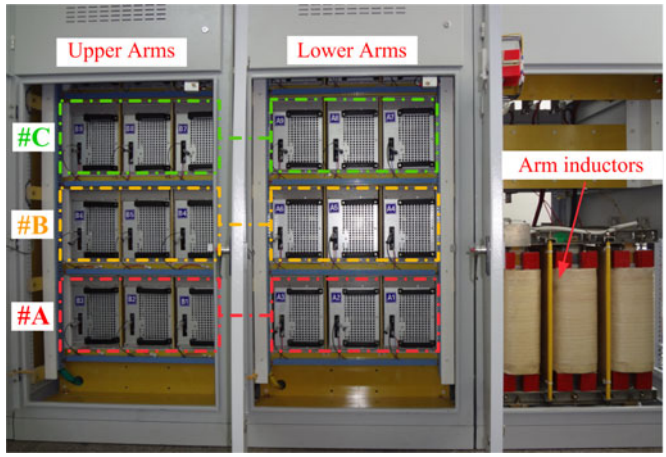

Fig. 7. Photograph of the laboratory prototype.

TABLE I
REFERENCE GENERATION ALGORITHM FOR THE UPPER ARM ($S = 0$)

	u_{uA}	u_{uB}	u_{uC}
$(u_{sA} > u_{sB})$ and $(u_{sA} > u_{sC})$	Blocked	$u_{oA} - u_{oB}$	$u_{oA} - u_{oC}$
$(u_{sB} > u_{sA})$ and $(u_{sB} > u_{sC})$	$u_{oB} - u_{oA}$	Blocked	$u_{oB} - u_{oC}$
$(u_{sC} > u_{sA})$ and $(u_{sC} > u_{sB})$	$u_{oC} - u_{oA}$	$u_{oC} - u_{oB}$	Blocked

TABLE II
REFERENCE GENERATION ALGORITHM FOR THE LOWER ARM ($S = 1$)

	u_{wA}	u_{wB}	u_{wC}
$(u_{sB} > u_{sA})$ and $(u_{sC} > u_{sA})$	Blocked	$u_{oB} - u_{oA}$	$u_{oC} - u_{oA}$
$(u_{sA} > u_{sB})$ and $(u_{sC} > u_{sB})$	$u_{oA} - u_{oB}$	Blocked	$u_{oC} - u_{oB}$
$(u_{sA} > u_{sC})$ and $(u_{sB} > u_{sC})$	$u_{oA} - u_{oC}$	$u_{oB} - u_{oC}$	Blocked

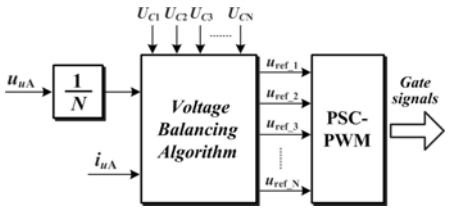

Fig. 6. Capacitor voltage balancing control during the ac-side start-up.

TABLE III
CIRCUIT PARAMETERS OF THE MMC PROTOTYPE

Quantity	Value
Number of SMs per arm	$N = 3$
Rated dc-side main voltage	$U_{dc} = 450$ V
Rated SM capacitor voltage	$U_{C(\text{rated})} = 150$ V
SM capacitance	$C_{SM} = 1867\ \mu$F
Bleeder resistor	$R_b = 9$ kΩ
Arm inductor	$L = 5$ mH
Fundamental frequency	$f_o = 50$ Hz
Switching frequency	$f_c = 2$ kHz

TABLE IV
CONTROL PARAMETERS USED FOR EXPERIMENTS

	Proportional gain	Integral gain	Balancing gain
DC-side start-up	$K_p = 15$ V/A	$K_i = 1800$ V/As	$K_b = 1.49$
AC-side start-up	$K_{p1} = 32$ V/A	$K_{i1} = 1600$ V/As	$K_{b1} = 2.2$

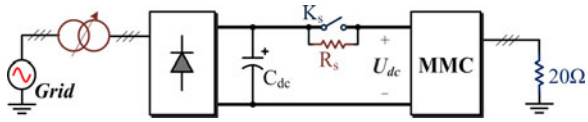

Fig. 8. System configuration used for dc-side start-up experiment.

As a result, by uncontrolled precharge from the dc-side main voltage, SM capacitor will have a 50% voltage difference away from the nominal value.[1]

C. Uncontrolled Precharge Process From the AC-Side Main Voltage

Fig. 3 presents the precharge process from the ac-side main voltage (e.g., the ac grid). Similarly, during this precharge process all the SMs are blocked. In terms of the three upper arms, at any time, one will be bypassed by the free-wheeling diode of S_2, whereas the other two will get charged through the free-wheeling diode of S_1. The arm that should be bypassed is determined by which phase voltage is the highest at that instant. Conversely, with respect to the three lower arms, the arm with the lowest phase voltage will be bypassed whereas the other two arms will get charged.

As a consequence, the maximum voltage that each SM capacitor can be precharged to is equal to the amplitude of the line-to-line ac voltage, that is

$$U_{C(\text{initial})} = \frac{\sqrt{3}U_S}{N} \tag{3}$$

[1] It should be noted that if there are redundant SMs [20], this voltage difference will be larger.

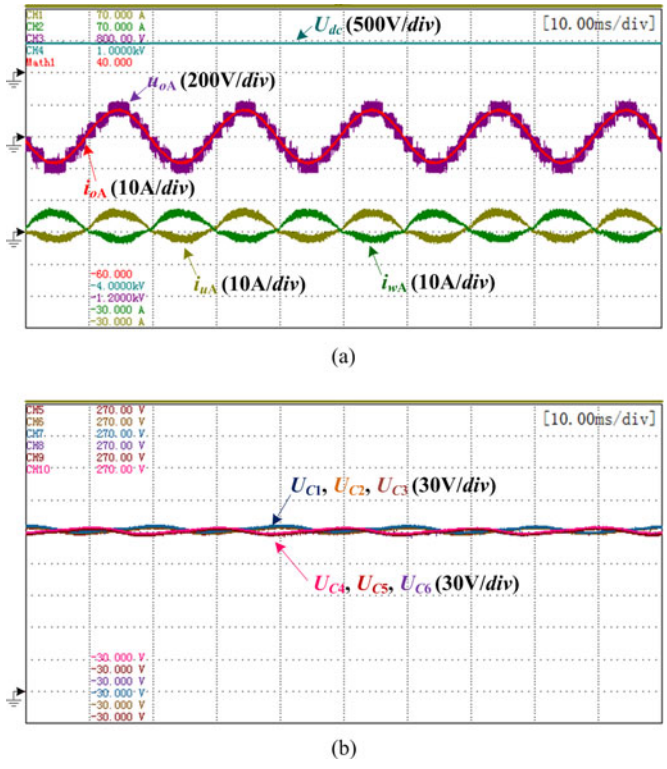

Fig. 9. Steady-state operation waveforms of MMC with dc-side main voltage: (a) dc-side main voltage $U_{\rm dc}$, ac-side voltage $u_{o\rm A}$, ac-side current $i_{o\rm A}$, lower-arm current $i_{w\rm A}$, and upper-arm current $i_{u\rm A}$; (b) upper-arm SM capacitor voltages $U_{C1}-U_{C3}$ and lower-arm SM capacitor voltages $U_{C4}-U_{C6}$.

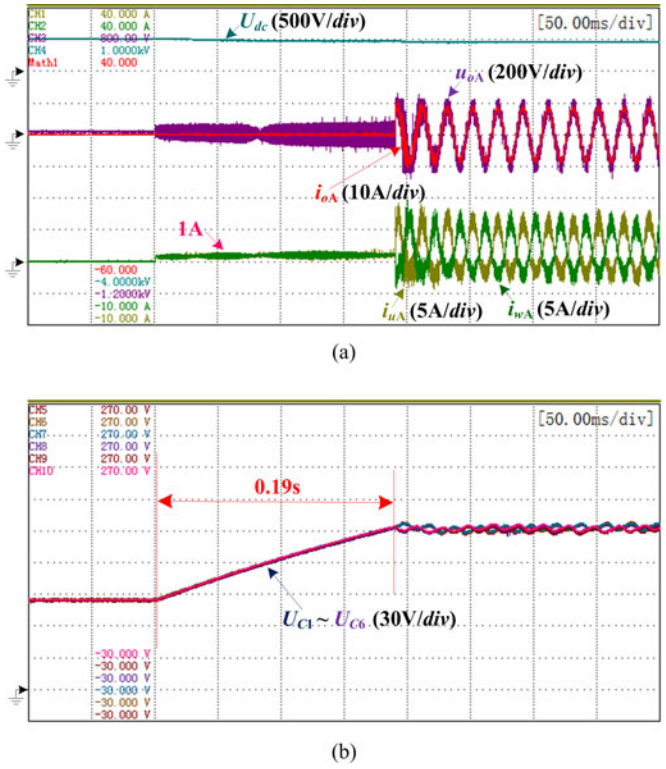

Fig. 10. Start-up performance of MMC from the dc-side main voltage: (a) dc-side main voltage $U_{\rm dc}$, ac-side voltage $u_{o\rm A}$, ac-side current $i_{o\rm A}$, lower-arm current $i_{w\rm A}$, and upper arm current $i_{u\rm A}$; (b) upper arm SM capacitor voltages $U_{C1}-U_{C3}$ and lower-arm SM capacitor voltages $U_{C4}-U_{C6}$.

where U_S is the amplitude of the phase voltage, and during normal operation of MMC, the following relationship exists

$$U_S = \mathrm{NM}\frac{U_{C(\mathrm{rated})}}{2} \tag{4}$$

where $M(0 \le M \le 1)$ denotes the modulation depth. Substituting (4) into (3) yields

$$U_{C(\mathrm{initial})} = \frac{\sqrt{3}M}{2}U_{C(\mathrm{rated})}. \tag{5}$$

Usually, *M* is around 0.9; hence, by uncontrolled precharge from the ac-side main voltage, there will be about 22% voltage difference on the rated value (see footnote 1).

III. Proposed Closed-Loop Precharge Control Methods

As MMC cannot be fully precharged through uncontrolled processes neither from the dc-side nor from the ac-side main voltage, further precharge methods must be adopted. The core idea of the proposed methods in this letter is to further charge MMC by regulating a constant charging current in a closed-loop manner, which can reduce the start-up time and eliminate initial current spikes. Note that once the uncontrolled precharge process ends, the contactors in Figs. 2 and 3 will be closed to bypass the limiting resistors.

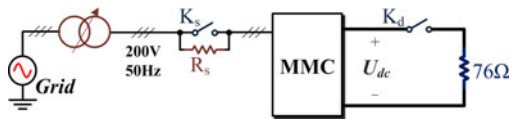

Fig. 11. System configuration used for ac-side start-up experiment.

A. Closed-Loop Control of the DC-Side Start-Up Current

Fig. 4 shows the proposed dc-side start-up control method, which takes phase **A** as an example. A PI regulator is utilized to make the circulating current i_{cA} constant by adjusting the output voltages of SMs. Moreover, the dc-side main voltage is used as feed-forward compensation at the output of the PI controller.

During this controlled precharge process, the ac current i_{oA} will be kept at zero and it can be obtained that

$$i_{u\rm A} = i_{w\rm A} = i_{c\rm A} = I_{C-\rm dc} \tag{6}$$

where $I_{C-\rm dc}$ is the reference value of the charging current. Hence, all the SMs will be charged by a constant arm current. Moreover, to maintain the SMs are equally charged during this start-up process, the capacitor balancing control is also taken into consideration by adjusting the reference of each SM as

$$u_{\mathrm{ref}\_i} = u_{\mathrm{ref}} - K_b\left(U_{Ci} - \frac{1}{2N}\sum_{i=1}^{2N}U_{Ci}\right) \times i_{c\rm A} \tag{7}$$

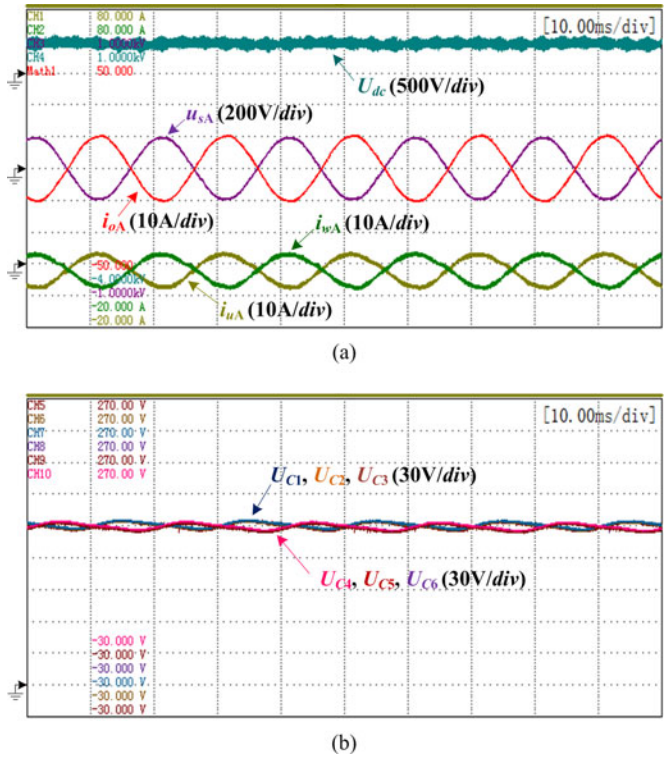

Fig. 12. Steady-state operation waveforms of MMC with ac-side main voltage: (a) dc-side main voltage $U_{\rm dc}$, ac-side voltage $u_{o\rm A}$, ac-side current $i_{o\rm A}$, lower-arm current $i_{w\rm A}$, and upper-arm current $i_{u\rm A}$; (b) upper-arm SM capacitor voltages $U_{C1}-U_{C3}$ and lower-arm SM capacitor voltages $U_{C4}-U_{C6}$.

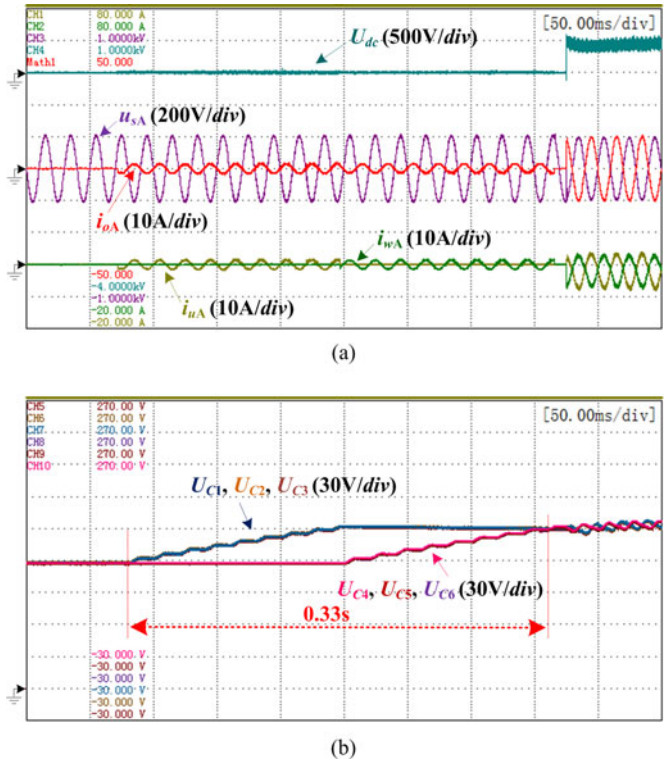

Fig. 13. Start-up performance of MMC from the ac-side main voltage: (a) dc-side main voltage $U_{\rm dc}$, ac-side voltage $u_{o\rm A}$, ac-side current $i_{o\rm A}$, lower-arm current $i_{w\rm A}$, and upper-arm current $i_{u\rm A}$; (b) upper-arm SM capacitor voltages $U_{C1}-U_{C3}$ and lower-arm SM capacitor voltages $U_{C4}-U_{C6}$.

where K_b denotes the proportional balancing gain, u_{ref_i} is the reference voltage of *i*th SM ($i = 1, 2, \ldots, 2N$), and U_{Ci} is the capacitor voltage of *i*th SM. As such, the SMs with voltages higher than the average will absorb less energy, and vice versa.

After all the SM voltages are charged to $U_{C(\mathrm{rated})}$, this procedure ends and MMC can enter into the normal operation. Assuming there is no power loss, the following equation can be obtained with the law of energy conservation:

$$\frac{1}{2}(2N)\,C_{\rm SM}\left[U_{C(\mathrm{rated})}^2 - U_{C(\mathrm{initial})}^2\right] = U_{\rm dc} I_{C-\rm dc} T_{\rm dc} \quad (8)$$

where $T_{\rm dc}$ is the charging time of this dc-side start-up process.

B. Closed-Loop Control of the AC-Side Start-Up Current

The ideal ac-side start-up control of MMC is to draw an ac current from the grid with constant rms value and unity power factor. Fig. 5 shows the block diagram of the proposed ac-side start-up control method. It employs the *d*–*q* decoupling current control scheme. The reference of the *d*-axis current is denoted as $I_{C-\rm ac}$, which determines the amplitude value of the precharge current during the start-up process. The *q*-axis current reference is set to zero so that the ac current of MMC during this precharge process will be under unity power factor with the grid voltage.

However, as (5) indicates that the SM capacitor voltages are below the rated value, the output voltage of MMC will be smaller than the grid voltage, which cannot be directly used to control the ac-side currents. To tackle this problem, the precharge control of MMC is performed by precharging the upper-arm SMs and the lower-arm SMs separately. When the switch S is turned to 0, the upper-arm currents i_{uj} ($j = A, B, C$) will be selected as the feedback. On the other hand, if $S = 1$, SMs in the lower arm will get charged by taking the lower-arm currents i_{wj} as feedback. A novel reference generation algorithm has been proposed to generate the voltage references of each arm, which samples and compares the three-phase grid voltages in real time. Table I shows the reference generation algorithm for the upper arms. Since the half-bridge SM can only output a positive voltage, the SMs in the arm with the highest phase voltage will be blocked while the references of the other two arms are obtained by subtracting the highest phase voltage with its own phase voltage. Similarly, as for the lower arms, the corresponding reference generation algorithm is shown in Table II. In this way, the input ac current can be well regulated with this closed-loop control method.

Assuming there is no power loss, it can be obtained that

$$\frac{1}{2}(6N)\,C_{\rm SM}\left[U_{C(\mathrm{rated})}^2 - U_{C(\mathrm{initial})}^2\right] = \frac{3}{2} U_S I_{C-\rm ac} T_{\rm ac} \quad (9)$$

where $T_{\rm ac}$ is the charging time of this ac-side start-up process.

Furthermore, the capacitor balancing control is also taken into consideration. As shown in Fig. 6, taking the upper arm of phase **A** as an example, the capacitor voltage balancing control

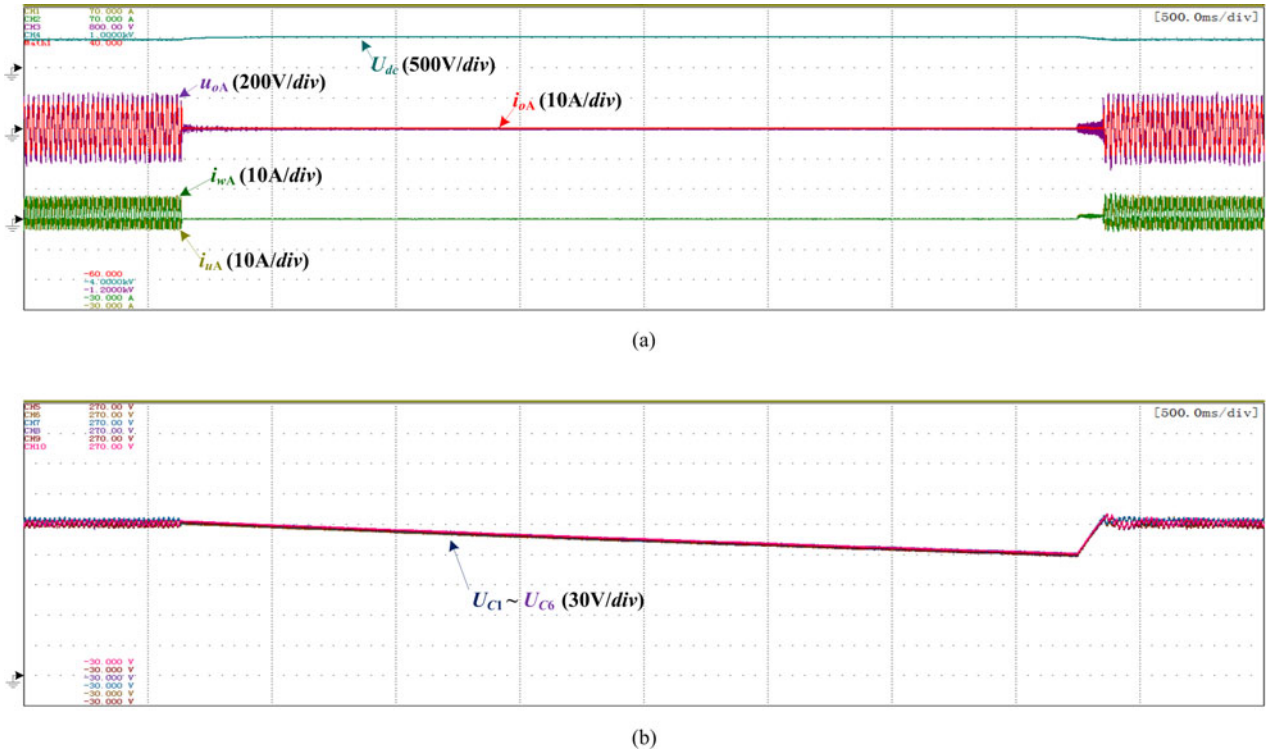

Fig. 14. DC-side start-up performances of MMC during restart: (a) dc-side main voltage U_{dc}, ac-side voltage $u_{o\mathrm{A}}$, ac-side current $i_{o\mathrm{A}}$, lower-arm current $i_{w\mathrm{A}}$, and upper-arm current $i_{u\mathrm{A}}$; (b) upper-arm SM capacitor voltages $U_{C1}-U_{C3}$ and lower-arm SM capacitor voltages $U_{C4}-U_{C6}$.

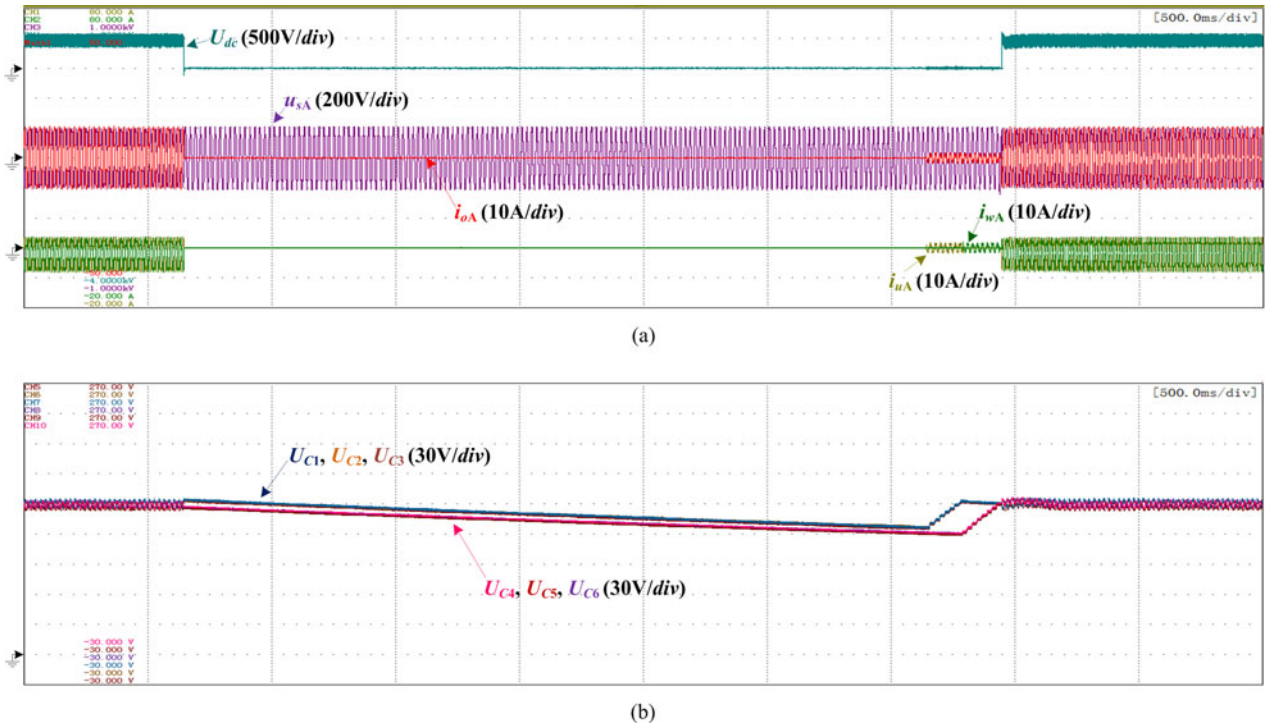

Fig. 15. AC-side start-up performances of MMC during restart: (a) dc-side main voltage U_{dc}, ac-side voltage $u_{o\mathrm{A}}$, ac-side current $i_{o\mathrm{A}}$, lower-arm current $i_{w\mathrm{A}}$, and upper-arm current $i_{u\mathrm{A}}$; (b) upper-arm SM capacitor voltages $U_{C1}-U_{C3}$ and lower-arm SM capacitor voltages $U_{C4}-U_{C6}$.

is expressed by

$$u_{\mathrm{ref}\_i} = K_{b1}\left(U_{Ci} - \frac{1}{N}\sum_{i=1}^{N} U_{Ci}\right) \times i_{u\mathrm{A}} \qquad (10)$$

where K_{b1} denotes proportional balancing gain, and $i = 1, 2 \ldots N$.

IV. Experimental Results

A. System Configuration

In order to verify the validity of the proposed start-up methods, a three-phase MMC prototype with three SMs per arm has been built, as shown in Fig. 7. The circuit parameters and operating conditions are listed in Table III. Note that each SM capacitor is paralleled with a 9-kΩ bleeder resistor. As for the controller, a TMS320F28335 DSP is used to generate the control references while an EP3C25Q240C8 FPGA is adopted to implement phase-shifted carrier (PSC) modulation [9] and send the PWM signals to SMs via optical fibers. Each SM is controlled by an EPM570T100 CPLD, which receives the PWM signals and sends back the monitored capacitor voltage. The control parameters are listed in Table IV.

As indicated by (8) and (9), the larger the reference value of the charging current ($I_{C-\mathrm{dc}}$ and $I_{C-\mathrm{ac}}$), the shorter the charging time will be. Choosing a larger reference value will accelerate the charging process, as long as this reference does not exceed the maximum allowable current limits of the system. However, in this letter, in order to clearly show the start-up processes, a much smaller charging current reference is selected in the following experiments to make MMC not precharged too fast.

B. DC-Side Start-Up Performance

Fig. 8 shows the system configuration of the dc-side start-up experiment, in which the MMC prototype is fed by a diode rectifier as the dc-side main voltage. The steady-state operation waveforms are shown in Fig. 9. Note that the output ac current is obtained by the math function of oscilloscope by subtracting the upper- and the lower-arm currents (i.e., $i_{oA} = i_{uA} - i_{wA}$). Meanwhile, the SM capacitor voltages $U_{C1} - U_{C6}$ are at the rated value of 150 V.

The performance of the proposed dc-side start-up scheme is shown in Fig. 10, where the reference value of the charging current $I_{C-\mathrm{dc}}$ is selected as 1 A. At first, the capacitor voltages can only be precharged to 83 V through uncontrolled process. After enabling the dc-side start-up control method, the arm currents i_{uA} and i_{wA} are regulated constant at 1 A without any inrush current, which confirms the effectiveness of the closed-loop controller. Once the SM capacitors are fully charged to 150 V, the ac-side current is generated and MMC turns into normal operation. The charging time of this process is measured as 0.19 s, which is basically same with the theoretical value calculated by (8). Besides, it can be seen that all the six capacitor voltages are kept equally charged during this start-up process with the voltage balancing algorithm.

C. AC-Side Start-Up Performance

Fig. 11 presents the system configuration for ac-side start-up experiment, in which the MMC prototype operates as a rectifier. The experimental results under steady-state are shown in Fig. 12. Note that some voltage ripple appears at the generated dc-side voltage U_{dc}, which is caused by the asynchronism switching of the SMs [13]. The SM capacitor voltages are with about 3% voltage fluctuation of the rated capacitor voltage (4.2 V with respect to 150 V).

Fig. 13 shows the performance of the proposed ac-side start-up scheme, and the charging current reference $I_{C-\mathrm{ac}}$ is set as 1.5 A. In the beginning, the capacitor voltages stay at 115 V by uncontrolled precharge of the ac-side main voltage. Then, by applying the proposed controller in Fig. 5, the upper-arm SMs and the lower-arm SMs are sequentially charged. After all the SM capacitor voltages reach 150 V, MMC starts its normal operation. As can be seen, during the whole start-up process, the obtained ac-side current i_{oA} is maintained constant, sinusoidal, without overshoot, and at unity power factor. In the meantime, the SM capacitor voltages are also well balanced. The total charging time of this ac-side start-up process is approximately 0.33 s, which is close to the theoretical value calculated by (9).

D. Restart Performances

Further experiments are performed to investigate the restart performances of the proposed start-up control methods. This is a very important feature of MMC especially when fast recovery after temporary fault is required [8]. In experiments, the operation of MMC is intentionally stopped for a while and then restarted. The experimental results are shown in Figs. 14 and 15. As each SM capacitor is paralleled with a 9-kΩ bleeding resistor, it can be seen that the capacitor voltages gradually decrease after MMC stops. And once MMC is ordered to get restart, the SM capacitors can be quickly recharged to the rated voltage and thereby MMC can immediately resume its normal operation. This illustrates that the proposed start-up control methods exhibit very fast restart performances. Moreover, the restart speed can be flexibly increased by selecting a higher charging current reference ($I_{C-\mathrm{dc}}$ and $I_{C-\mathrm{ac}}$).

V. Conclusion

In this letter, two closed-loop control methods are proposed to precharge MMC with a constant charging current from the dc-side and the ac-side main voltage, respectively. The advantages of the proposed methods are: requiring no auxiliary power supply, elimination of inrush current, reduced charging time, voltage balancing of the SM capacitors, and the capability of fast restart. Moreover, due to the easy implementation and robustness of closed-loop control, the proposed start-up methods can be applied to any MMC application regardless of the number of SMs and power ratings. Finally, the validity and effectiveness of the proposed methods have been confirmed by experiments based on a three-phase MMC prototype in the laboratory.

REFERENCES

[1] S. Kouro, M. Malinowski, K. Gopakumar, J. Pou, L. G. Franquelo, B. Wu, J. Rodriguez, M. A. Perez, and J. I. Leon, "Recent advances and industrial applications of multilevel converters," *IEEE Trans. Ind. Electron.*, vol. 57, no. 8, pp. 2553–2580, Aug. 2010.

[2] N. Flourentzou, V. G. Agelidis, and G. Demetriades, "VSC based HVDC power transmission systems: An overview," *IEEE Trans. Power Electron.*, vol. 24, no. 3, pp. 592–602, Mar. 2009.

[3] H. Akagi, "Classification, terminology, and application of the modular multilevel cascade converter (MMCC)," *IEEE Trans. Power Electron.*, vol. 26, no. 11, pp. 3119–3130, Nov. 2011.

[4] A. Lesnicar and R. Marquardt, "An innovative modular multilevel converter topology suitable for a wide power range," presented at the IEEE Power Tech Conf., Bologna, Italy, Jun. 23–26, 2003, vol. 3.

[5] A. Antonopoulos, L. Angquist, and H.-P. Nee, "On dynamics and voltage control of the modular multilevel converter," presented at the *13th Eur. Conf. Power Electron. Appl.*, Barcelona, Spain, Sep. 8–10, 2009.

[6] S. Rohner, S. Bernet, M. Hiller, and R. Sommer, "Modulation, losses, and semiconductor requirements of modular multilevel converters," *IEEE Trans. Ind. Electron.*, vol. 57, no. 8, pp. 2633–2642, Aug. 2010.

[7] S. Shao, P.W. Wheeler, J. C. Clare, and A. J. Watson, "Fault detection for modular multilevel converters based on sliding mode observer," *IEEE Trans. Power Electron.*, vol. 28, no. 11, pp. 4867–4872, Nov. 2013.

[8] X. Li, Q. Song, W. Liu, H. Rao, S. Xu, and L. Li, "Protection of nonpermanent faults on dc overhead lines in MMC-based HVDC systems," *IEEE Trans. Power Del.*, vol. 28, no. 1, pp. 483–490, Jan. 2013.

[9] B. Li, R. Yang, D. Xu, G. Wang, W. Wang, and D. Xu, "Analysis of the phase-shifted carrier modulation for modular multilevel converters," *IEEE Trans. Power Electron.*, to be published.

[10] M. Hagiwara, K. Nishimura, and H. Akagi, "A medium-voltage motor drive with a modular multilevel PWM inverter," *IEEE Trans. Power Electron.*, vol. 25, no. 7, pp. 1786–1799, Jul. 2010.

[11] Z. Li, P. Wang, Z. Chu, H. Zhu, Y. Luo, and Y. Li, "An inner current suppressing method for modular multilevel converters," *IEEE Trans. Power Electron.*, vol. 28, no. 11, pp. 4873–4879, Nov. 2013.

[12] K. Wang, Y. Li, Z. Zheng, and L. Xu, "Voltage balancing and fluctuation-suppression method of floating capacitors in a new modular multilevel converter," *IEEE Trans. Ind. Electron.*, vol. 60, no. 5, pp. 1943–1954, May 2013.

[13] H. Peng, M. Hagiwara, and H. Akagi, "Modeling and analysis of switching-ripple voltage on the DC link between a diode rectifier and a modular multilevel cascade inverter (MMCI)," *IEEE Trans. Power Electron.*, vol. 28, no. 1, pp. 75–84, Jan. 2013.

[14] K. Li and C. Zhao, "New technologies of modular multilevel converter for VSC-HVDC application", in *Proc. Asia-Pacific Power and Energy Eng. Conf.*, 2010, pp. 1–4.

[15] A. Das, H. Nademi, and L. Norum, "A method for charging and discharging capacitors in modular multilevel converter," in *Proc. Conf. IEEE Ind. Electronics. Society.*, 2011, pp. 1058–1062.

[16] K. Shi, F. Shen, D. Lv, P. Lin, M. Chen, and D. Xu, "A novel start-up scheme for modular multilevel converter," in *Proc. Conf. IEEE Energy Convers. Congr. Expo.*, 2012, pp. 4180–4187.

[17] Y. Xue, Z. Xu, and G. Tang, "Self-start control with grouping sequentially precharge for the C-MMC-based HVDC system," *IEEE Trans. Power Del.*, vol. 29, no. 1, pp. 187–198, Feb. 2014.

[18] M. Glinka, "Prototype of multiphase modular-multilevel-converter with 2 MW power rating and 17-level-output-voltage," in *Proc. IEEE Power Electron. Spec. Conf.*, Aachen, Germany, vol. 4, pp. 2572–2576, Jun. 2004.

[19] T. Modeer, S. Norrga, and H.-P. Nee, "High-voltage tapped-inductor buck converter auxiliary power supply for cascaded converter submodules," in *Proc. Conf. IEEE Energy Convers. Congr. Expo.*, 2012, pp. 19–25.

[20] G. Konstantinou, J. Pou, S. Ceballos, and V. G. Agelidis, "Active redundant submodule configuration in modular multilevel converters," *IEEE Trans. Power Del.*, vol. 28, no. 4, pp. 2333–2341, Oct. 2013.